Am J Transl Res 2026;18(6):5291-5302
www.ajtr.org /ISSN:1943-8141/AJTR0173930

Original Article

Reserpine-induced hypotension through catecholamine and RAAS/nitric oxide/endothelin dysregulation

Ya Mo, Ming Jiang, Hong-Lei Zhou, Jia-Wen Wang, Rui Wang

Shanghai Key Laboratory of New Drug Design, School of Pharmacy, East China University of Science and Technology, Shanghai 200237, P. R. China

Received May 10, 2026; Accepted June 8, 2026; Epub June 15, 2026; Published June 30, 2026

Abstract: Objective: This study aims to investigate the mechanisms underlying reserpine-induced hypotension. Methods: A rat model of hypotension was established by reserpine administration, followed by levodopa (L-DOPA) intervention. Arterial blood pressure, histopathologic changes in the heart and kidneys, the levels of norepinephrine (NE), the renin-angiotensin-aldosterone system (RAAS), and endothelial function markers were systematically evaluated. Results: Reserpine significantly lowered blood pressure and caused myofibrillar disarray, tubular epithelial degeneration, and elevated biomarkers of cardiac and renal injury. These pathologic changes were attributable primarily to depletion of NE and dysregulation of vasoactive regulatory systems. L-DOPA treatment restored NE and vasoactive mediator levels and markedly ameliorated hypotension and cardiorenal injury. Conclusion: Reserpine induces hypotension and cardiorenal injury through suppression of the catecholamine system, accompanied by dysregulation of the RAAS and nitric oxide/endothelin (NO/ET) system, whereas L-DOPA attenuates these pathologic changes.

Keywords: Hypotension, reserpine, cardio-renal injury, norepinephrine, RAAS, NO/ET system

Introduction

Hypotension is generally defined as a systolic blood pressure (SBP) below 90 mmHg and a diastolic blood pressure (DBP) below 60 mmHg [1]. Neurogenic hypotension is a distinct subtype of hypotension defined by decreased blood pressure resulting from dysfunction of the autonomic nervous system, particularly the sympathetic nervous system [2]. Neurogenic hypotension is commonly observed in elderly individuals and patients with autonomic dysfunction. Compared to primary hypotension, this condition features a far more intricate pathogenesis. Consequently, its clinical consequences are inherently more severe, frequently culminating in the hypoperfusion of critical target organs such as the heart, brain, and kidneys. Reduced cardiac perfusion may result in palpitations, fatigue, and even myocardial infarction, whereas cerebral ischemia can cause dizziness, headache, and severe cases of ischemic stroke [3, 4]. Reduced renal blood flow can also impair kidney function, leading to systemic edema, oliguria, and proteinuria [5]. Collectively, these findings highlight neurogenic hypotension as a public health concern that warrants greater clinical attention.

Blood pressure regulation is highly complex and involves multiple interconnected systems, including the sympathetic nervous system (SNS), RAAS, NO/ET system, as well as inflammatory and immune systems [6]. Current therapeutic strategies for neurogenic hypotension focus primarily on the sympathetic nervous system, including norepinephrine reuptake inhibitors [7, 8], α1-adrenergic receptor agonists and norepinephrine precursors. Although these agents exhibit favorable short-term efficacy, their long-term efficacy remains suboptimal, and their use is often associated with substantial adverse effects and poor patient adherence, thereby limiting their clinical applicability [9, 10]. Therefore, the development of safer and more effective therapeutic agents remains an urgent priority. However, the underlying pathophysiologic mechanisms of neurogenic

https://doi.org/10.62347/ZWLA9582

hypotension remain incompletely understood, which has substantially hindered the progress of novel drug development. In this context, a comprehensive investigation of the mechanisms involved in neurogenic hypotension may provide important mechanistic insight for the development of new therapeutic strategies.

Reserpine is a well-established antihypertensive agent that exerts antihypertensive effects by targeting the vesicular monoamine transporter (VMAT). By inhibiting the transport of catecholamine neurotransmitters, including norepinephrine and dopamine, into synaptic vesicles, reserpine suppresses their storage in sympathetic nerve terminals. This reduction in peripheral sympathetic activity subsequently promotes vasodilation and ultimately results in blood pressure reduction [11]. Reserpine-induced hypotension closely mimics the clinical manifestations of neurogenic hypotension. Previous studies have demonstrated that reserpine can successfully establish a stable hypotensive rat model [12]. Building upon these findings, the present study systematically investigated the mechanisms underlying reserpine-induced hypotension from multiple perspectives, including the SNS, RAAS, and NO/ET system. This research provides a robust foundation for preclinical efficacy evaluation.

Nevertheless, several limitations remained in previous studies. First, conventional reserpine-induced hypotension models generally require a relatively long induction period of 3-7 weeks, resulting in relatively low modeling efficiency. Second, most studies have focused primarily on alterations in the SNS, whereas the interactions among multiple blood pressure regulatory systems, including the RAAS and NO/ET system, have not been systematically investigated. In addition, assessment of cardiac and renal injury secondary to hypotension remains insufficient. To address these limitations, the present study established a reserpine-induced hypotensive rat model characterized by a shorter induction period and improved stability. The possible mechanisms underlying reserpine-induced hypotension were systematically investigated from multiple perspectives, including the SNS, RAAS, and NO/ET system. Furthermore, histopathologic examination combined with evaluation of cardiac and renal function was performed to comprehensively characterize organ injury associated with hypotension. These findings provide a more comprehensive experimental basis for mechanistic studies of neurogenic hypotension and for the development of novel therapeutic agents.

Materials and methods

Animals

Eight-week-old male SPF Wistar rats [Shanghai BK Laboratory Animal Co., Ltd., Shanghai, China], weighing 190 ± 10 g, were housed at 20-26°C with a relative humidity of 50%-60% under a 12 h light/dark cycle, with free access to food and water. The experimental protocol was approved by the Bioethics Committee of the East China University of Science and Technology (Ethics Approval: ECUST-2026-110).

Animal grouping and model establishment

After one week of acclimatization, the rats underwent 7 days of tail-cuff blood pressure training. Animals were then randomly assigned to a control group, model group, and L-DOPA group, with no significant differences in baseline blood pressure or heart rate among the groups. From days 1 to 7, rats in the model and L-DOPA (HY-N0304; MedChemExpress, USA) groups received reserpine (H12020905, Tianjin KingYork Pharmaceutical Co., Ltd., China) suspension by oral gavage at a dose of 5 mg/kg/day to induce hypotension. Beginning on day 8, the modeling protocol was changed to intraperitoneal injection of reserpine (0.5 mg/kg) once every 2 days. During this period, rats in the control and model groups were administered daily gavage of distilled water, whereas rats in the L-DOPA group received L-DOPA at 30 mg/kg/day by gavage. The administration volume was maintained at 5 mL/kg. Baseline blood pressure was measured one day before model induction, and subsequent measurements were performed on days 7, 11, and 15 during the experimental period. All rats were sacrificed for sample collection on day 16. Prior to euthanasia, the animals were deeply anesthetized with isoflurane until the complete loss of reflex activity was achieved, followed by cervical dislocation to minimize animal suffering as much as possible.

Tail-cuff blood pressure measurement

Blood pressure was measured primarily using the tail-cuff method, which is based on occlusion and release of the tail artery in conscious rats. Prior to measurement, the environment was kept quiet and comfortable. Rats were placed in a restrainer with their tails threaded through the tail cuff to ensure a relaxed posture, and the sensor was positioned at the base of the tail. The device was then activated to automatically inflate and measure blood pressure. Each rat was measured five times at 30-second intervals, and the average of the five readings was recorded as the blood pressure value for that session.

Hematoxylin and eosin staining

After deparaffinization, tissue sections were stained in hematoxylin solution for 8 minutes, followed by a 10-minute wash under running tap water. The sections were then differentiated with 0.5% acid alcohol for 10 seconds and washed under running water for an additional 10 minutes. Subsequently, the sections were counterstained in eosin solution for 10 seconds. After dehydration and clearing, the sections were mounted using neutral resin and coverslipped for microscopic analysis.

Enzyme-linked immunosorbent assay

Rat plasma samples collected from the abdominal aorta were centrifuged at 3200 rpm for 15 min at 4°C, and the supernatants were collected for analysis. Cardiac and renal tissues were minced, homogenized in sterile PBS, and centrifuged at 5000×g for 10 min at 4°C, after which the supernatants were harvested. According to the ELISA kits, myocardial injury markers, including brain natriuretic peptide (H166-1-2, Nanjing Jiancheng Bioengineering Institute, China), creatine kinase-MB (H197-1-2, Nanjing Jiancheng Bioengineering Institute, China), and cardiac troponin T (H149-2-2, Nanjing Jiancheng Bioengineering Institute, China) were quantified using ELISA kits according to the manufacturer's instructions. Renal injury was assessed by measuring cystatin C (H336-1-2, Nanjing Jiancheng Bioengineering Institute, China). Vasoactive factors including Angiotensin II (E-EL-H0326, Elabscience, China), aldosterone (E-EL-0070, Elabscience, China), and endothelin-1 (E-EL-R1458, Elabscience, China), were determined using ELISA kits following the recommended protocols.

Assessment of blood urea nitrogen and serum creatinine levels

Plasma urea nitrogen (BUN) levels were measured using a commercial kit (C013-2-1, Nanjing Jiancheng Bioengineering Institute, China) based on the diacetyl monoxime method. Chromogenic reagent was added to the plasma samples. Then the mixtures were precisely heated in a boiling water bath to develop color. After cooling to room temperature, absorbance was measured at 520 nm. The BUN concentrations were calculated using a standard curve. Plasma creatinine levels were determined using a commercial kit (C011-2-1, Nanjing Jiancheng Bioengineering Institute, China) following the Jaffe reaction. Plasma samples were first treated with a protein precipitant to remove interfering substances. The supernatants were mixed with alkaline picrate reagent at room temperature to induce color development. Absorbance was subsequently measured at 510 nm, and creatinine concentrations were quantified using a standard curve.

LC-MS/MS analysis of NE levels

Collected plasma samples were processed by protein precipitation and derivatization prior to LC-MS/MS analysis. For tissue samples, the heart and kidneys were minced and homogenized in sterile PBS. Tissue homogenates were centrifuged at 5,000×g for 10 minutes at 4°C. After centrifugation, the supernatants were harvested. These supernatants were then subjected to the same protein precipitation and derivatization procedures as the plasma samples. Following sample preparation, the prepared samples were injected into the LC-MS/MS system. Chromatographic separation was achieved using a C18 column (2.1 × 100 mm, 1.7 μm) maintained at 40°C with a flow rate of 0.3 mL/min. Mobile phase A consisted of 0.1% formic acid in water, while mobile phase B consisted of acetonitrile, and gradient elution was applied. Mass spectrometric detection was performed in positive electrospray ionization mode using multiple reaction monitoring. The transition ion for norepinephrine was monitored at m/z 170.1→152.1. The spray voltage and ion source temperature were set at 4500 V and 550°C, respectively.

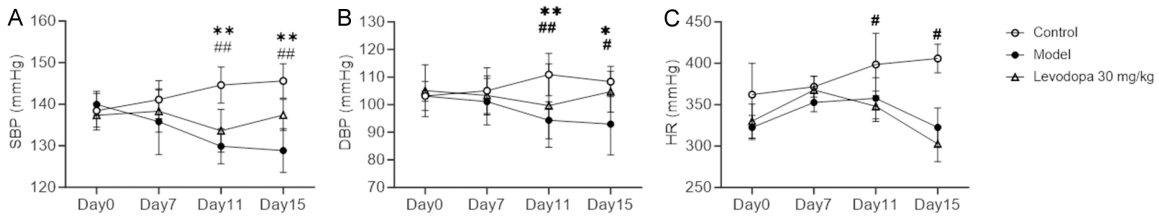

Figure 1. Effect of reserpine on blood pressure and heart rate of Wistar rats. A. SBP (systolic blood pressure); B. DBP (diastolic blood pressure); C. HR (heart rate). mean ± SD, n=8. $^{\#}P<0.05$, $^{\#\#}P<0.01$ *vs*. Control group; $^{*}P<0.05$, $^{**}P<0.01$ *vs*. Model group.

Western blot assay

Heart and kidney tissues were excised, minced, and homogenized, followed by lysis in RIPA buffer for protein extraction. Protein concentrations were quantified using a BCA assay kit. Equal amounts of protein were separated on 12% SDS-PAGE gels at 120 V and subsequently transferred onto PVDF membranes. The membranes were blocked with skimmed milk for 2 hours and then incubated overnight at 4°C with tyrosine hydroxylase (58844, Cell Signaling Technology, USA), dopa decarboxylase (13561, Cell Signaling Technology, USA), dopamine β-hydroxylase (abs116197, Absin, China), the norepinephrine transporter (ab41559, Abcam, USA), endothelial nitric oxide synthase (32027S, Cell Signaling Technology, USA), endothelin-1 (14069S, Cell Signaling Technology, USA), and GAPDH (60004-1-Ig, Proteintech, USA). After washing with TBST, membranes were incubated at room temperature for 2 hours with the corresponding HRP-conjugated secondary antibodies (RGAM001, Proteintech, USA; RGAR001, Proteintech, USA) on a shaker. Protein bands were detected using chemiluminescent reagents.

NO detection

The nitric oxide (NO) levels were measured using a commercial colorimetric assay kit (E-BC-K035-M, Elabscience, China). Nitrates were first completely reduced to nitrites using a reduction agent. Griess reagent was subsequently added, and diazotization was performed at room temperature, yielding a pink azo dye complex. Absorbance was measured at 540 nm, and total NO concentrations were calculated using a standard calibration curve.

Statistical analysis

Data analysis and graphing were performed using GraphPad Prism 10.0. All experimental results are presented as mean ± SD. Statistical comparisons among groups were conducted using one-way ANOVA in IBM SPSS 26, followed by LSD *post hoc* tests for multiple comparisons. Values with $P<0.05$ were defined as being significant.

Results

Reserpine successfully induced a hypotension model in Wistar rats

The changes in blood pressure during reserpine-induced hypotension modeling are shown below. Starting from day 11, a significant decrease in SBP was observed in the model group relative to the control group ($P<0.01$). In contrast, intervention with L-DOPA significantly reversed this trend, increasing both SBP and DBP compared to the model group ($P<0.01$; $P<0.01$) (**Figure 1**). On day 15, SBP, DBP, and HR (heart rate) were significantly reduced in the model group compared to the control group, with SBP decreased by approximately 20 mmHg ($P<0.01$) and DBP decreased by approximately 15 mmHg ($P<0.05$) (**Figure 2**). L-DOPA administration significantly restored SBP and DBP toward baseline levels ($P<0.01$; $P<0.05$). These results indicate that a 15-day reserpine-induced hypotension model in Wistar rats was successfully established.

Reserpine-induced myocardial injury in Wistar rats

Dysregulated blood pressure can induce structural injury in cardiac and renal tissues. Exce-

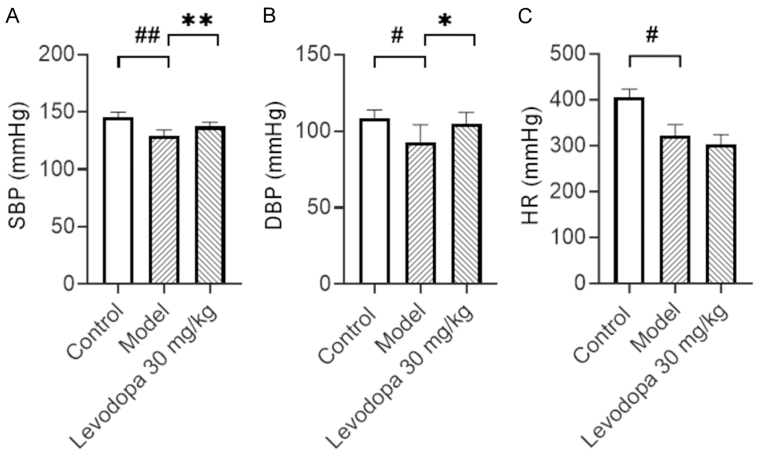

Figure 2. Effect of reserpine on blood pressure and heart rate of Wistar rats on day 15. A. SBP (systolic blood pressure); B. DBP (diastolic blood pressure); C. HR (heart rate). mean ± SD, n=8. $^{\#}P<0.05$, $^{\#\#}P<0.01$ *vs*. Control group; $^{*}P<0.05$, $^{**}P<0.01$ *vs*. Model group.

ssive reductions in blood pressure have been reported to impair myocardial contractility and reduce perfusion to the heart and kidneys, ultimately resulting in injury and apoptosis of cardiomyocytes and renal tubular epithelial cells [13]. Hematoxylin and eosin (H&E) staining showed that myocardial cells in the control group were regularly arranged, with well-defined striations and evenly distributed cytoplasm (**Figure 3A**). In contrast, the model group displayed pronounced myofibrillar disorganization, loss of striations, nuclear pyknosis, and indistinct nucleoli. L-DOPA treatment partially restored myocardial architecture, with more orderly striations and largely preserved nuclear morphology. These findings indicate that reserpine-induced hypotension caused structural damage to cardiac tissue in Wistar rats, whereas L-DOPA treatment effectively alleviated these pathologic alterations. Structural alterations in the heart and kidney are often accompanied by functional impairment, thereby exacerbating disease progression [14]. After L-DOPA administration, plasma Brain natriuretic peptide (BNP) and creatine kinase-MB (CK-MB) concentrations were significantly reduced ($P<0.05$; $P<0.05$) (**Figure 3B** and **3C**). BNP, CK-MB, and cardiac troponin T (cTn-T) are well-established biomarkers of cardiac dysfunction. Compared to the control group, plasma BNP and cTn-T levels were significantly elevated in the model group ($P<0.01$; $P<0.05$) (**Figure 3B** and **3D**). These findings indicate that reserpine-induced hypotension leads to myocardial injury and impaired cardiac contractile function, both of which were effectively attenuated following L-DOPA administration.

Reserpine-induced renal injury in Wistar rats

H&E staining revealed normal renal histology in the control group, with clear glomerular structures and regularly arranged renal tubules (**Figure 4A**). In contrast, rats in the model group exhibited marked pathologic alterations, including dilation of the proximal tubular lumen, degeneration of tubular epithelial cells, nuclear loss, and cellular desquamation. After L-DOPA treatment, these structural abnormalities were markedly alleviated, and both glomerular and tubular morphology appeared largely preserved. These findings indicate that reserpine-induced hypotension leads to renal structural injury in Wistar rats, whereas L-DOPA treatment effectively attenuates these changes. Renal structural injury is often associated with impaired glomerular filtration function. BUN and creatinine (Cre) are commonly used biomarkers of renal function, and elevated levels generally reflect reduced glomerular filtration rate. However, significant changes in these indices typically occur only after substantial renal injury. No significant differences in plasma BUN or Cre levels were observed among the groups, possibly due to insufficient duration of model establishment to cause severe renal dysfunction (**Figure 4B** and **4C**). In comparison with BUN and Cre, cystatin C (Cys-C), which is exclusively cleared by the kidneys, is regarded as a more sensitive biomarker of early renal dysfunction. Plasma Cys-C levels were significantly increased in the model group compared to the control group ($P<0.01$), indicating impaired renal filtration function in hypotensive rats (**Figure 4D**). Notably, L-DOPA treatment significantly decreased plasma Cys-C levels ($P<0.01$), suggesting that it effectively alleviated hypotension-induced renal dysfunction.

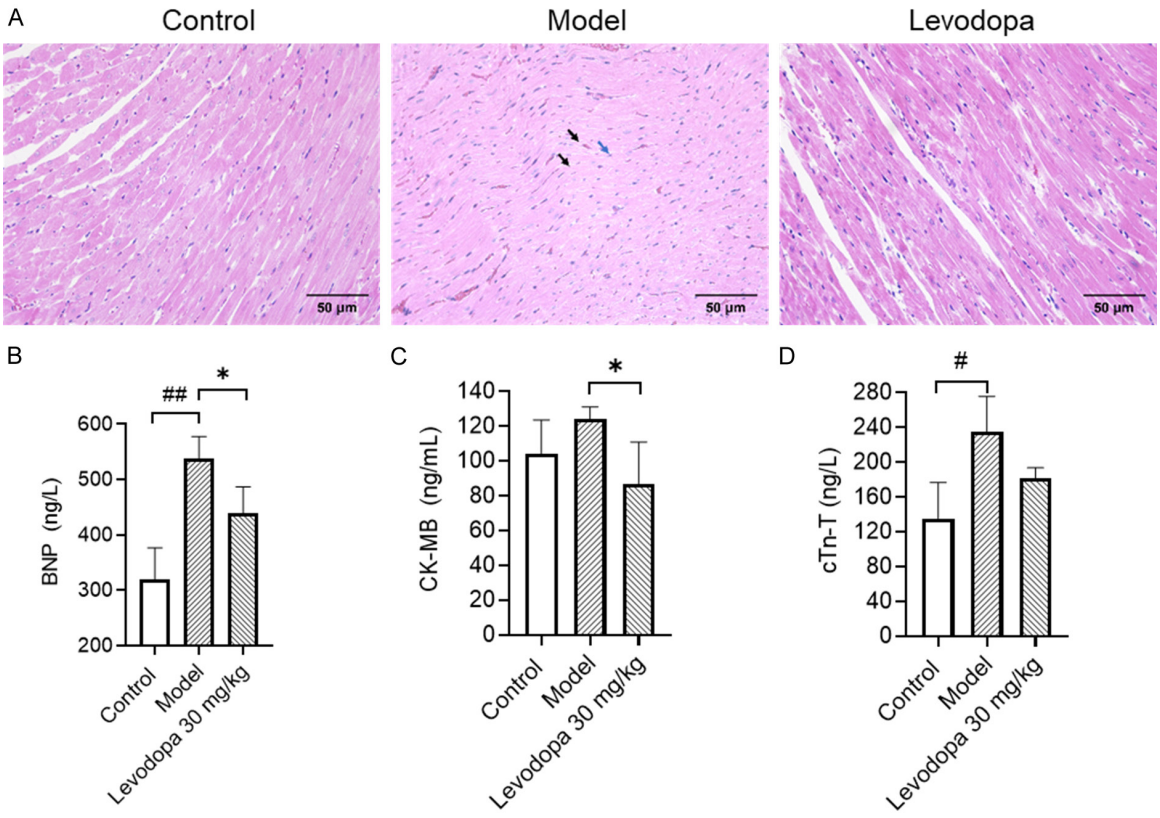

Figure 3. Effect of reserpine on myocardial injury of Wistar rats. A. H&E staining results of cardiac tissue (200×); Black arrows indicate disordered arrangement of myofibrils and disappearance of striations; Blue arrows indicate pyknotic nuclei and unclear nucleoli. B. Plasma BNP level; C. Plasma CK-MB level; D. Plasma cTn-T level. mean ± SD, n=3, scale bar=50 μm. $^{\#}P<0.05$, $^{\#\#}P<0.01$ *vs*. Control group; $^{*}P<0.05$ *vs*. Model group.

Reserpine inhibits norepinephrine synthesis and reuptake in Wistar rats

Previous studies have demonstrated that reserpine depletes NE in sympathetic nerve terminals, thereby inhibiting sympathetic neurotransmission, promoting vasodilation, and ultimately reducing blood pressure [15]. NE levels in the plasma as well as in cardiac and renal tissues were significantly decreased in the model group compared to the control group ($P<0.05$; $P<0.01$; $P<0.01$). L-DOPA administration significantly restored NE levels in both plasma and tissues (**Figure 5**).

Relative to the control group, tyrosine hydroxylase (TH) expression in the cardiac and renal tissues of rats in the model group was significantly increased, whereas L-DOPA administration markedly reduced TH levels (**Figure 6A** and **6B**). As the rate-limiting enzyme in NE biosynthesis, TH is subject to negative feedback regulation by NE. Therefore, the elevated TH expression observed in the model group may represent a compensatory response to NE depletion. Conversely, the expression levels of dopa decarboxylase (DDC) and dopamine β-hydroxylase (DBH), two key enzymes involved in NE synthesis, were significantly decreased in the cardiac and renal tissues of the model group compared to the control group (**Figure 6A** and **6B**).

In physiologic states, most NE released into the synaptic cleft is transported back into the cytoplasm through the norepinephrine transporter (NET) and subsequently repackaged into synaptic vesicles for storage. To further investigate NE reuptake, NET expression was evaluated in cardiac and renal tissues. NET expression in the model group was reduced to varying degrees relative to the control group. After L-DOPA administration, NET expression was par-

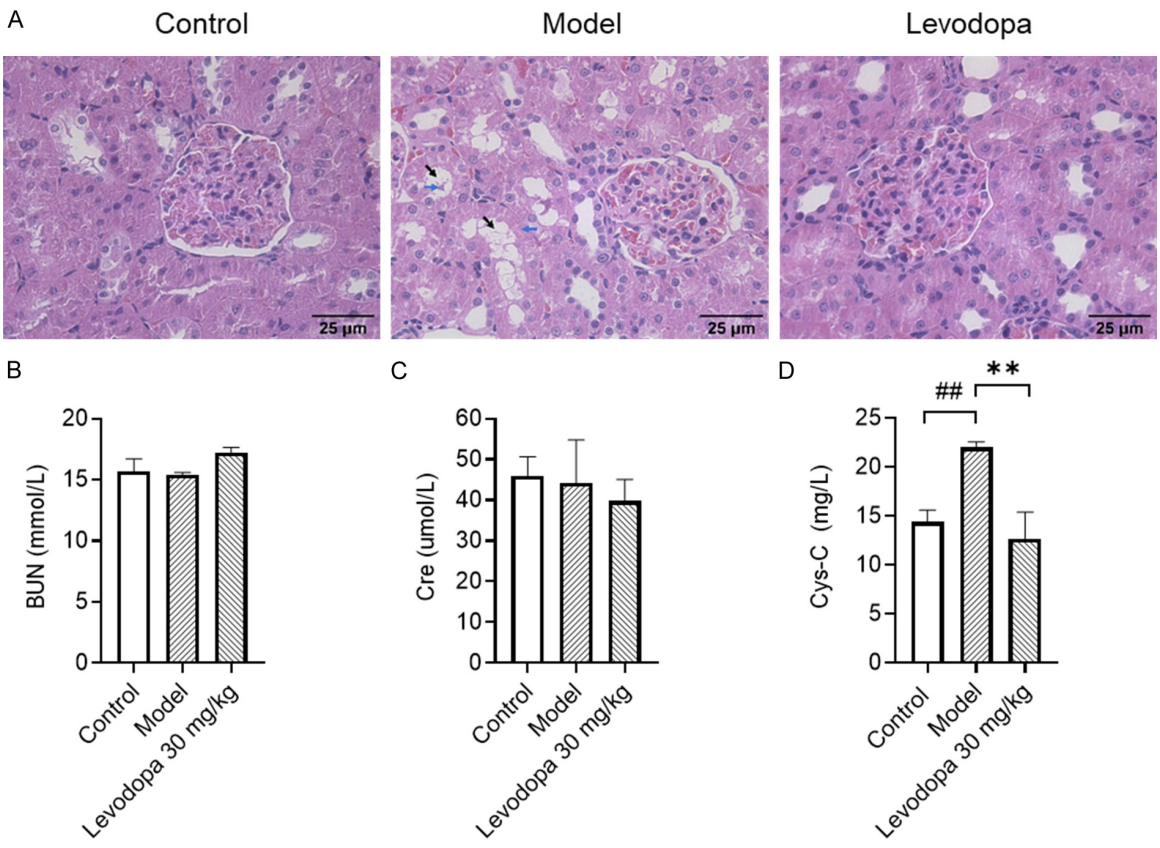

Figure 4. Effect of reserpine on renal injury of Wistar rats. A. H&E staining results of renal tissue (400×); Black arrows indicate the enlargement of the proximal convoluted tubule lumen; Blue arrows indicate renal tubular cell degeneration, loss of cell nuclei, and cell detachment; B. Plasma BUN level; C. Plasma Cre level; D. Plasma Cys-C level. mean ± SD, n=3, scale bar=25 μm. $^{\#\#}P<0.01$ *vs*. Control group; $^{**}P<0.01$ *vs*. Model group.

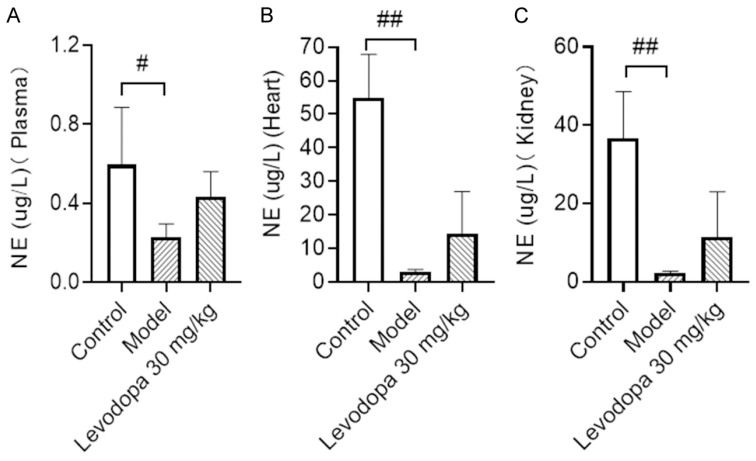

Figure 5. Effect of reserpine on NE level of Wistar rats. A. Plasma NE level; B. Cardiac tissue NE level; C. Renal tissue NE level. mean ± SD, n=3. $^{\#}P<0.05$, $^{\#\#}P<0.01$ vs. Control group.

tially restored in both cardiac and renal tissues (**Figure 7**).

Reserpine inhibits the activation of the RAAS system in Wistar rats

Considering the interaction between sympathetic regulation and renal endocrine function, we further evaluated changes in the RAAS. RAAS is one of the major mechanisms involved in blood pressure regulation. Short-term activation of the RAAS contributes to the maintenance of cardiac output during hypotension by promoting sodium and water retention as well as vasoconstriction [16]. Angiotensin II (Ang II) and aldosterone (ALD), two key components of the RAAS, are widely recognized as classic biomarkers of its activation [17, 18]. The results showed that

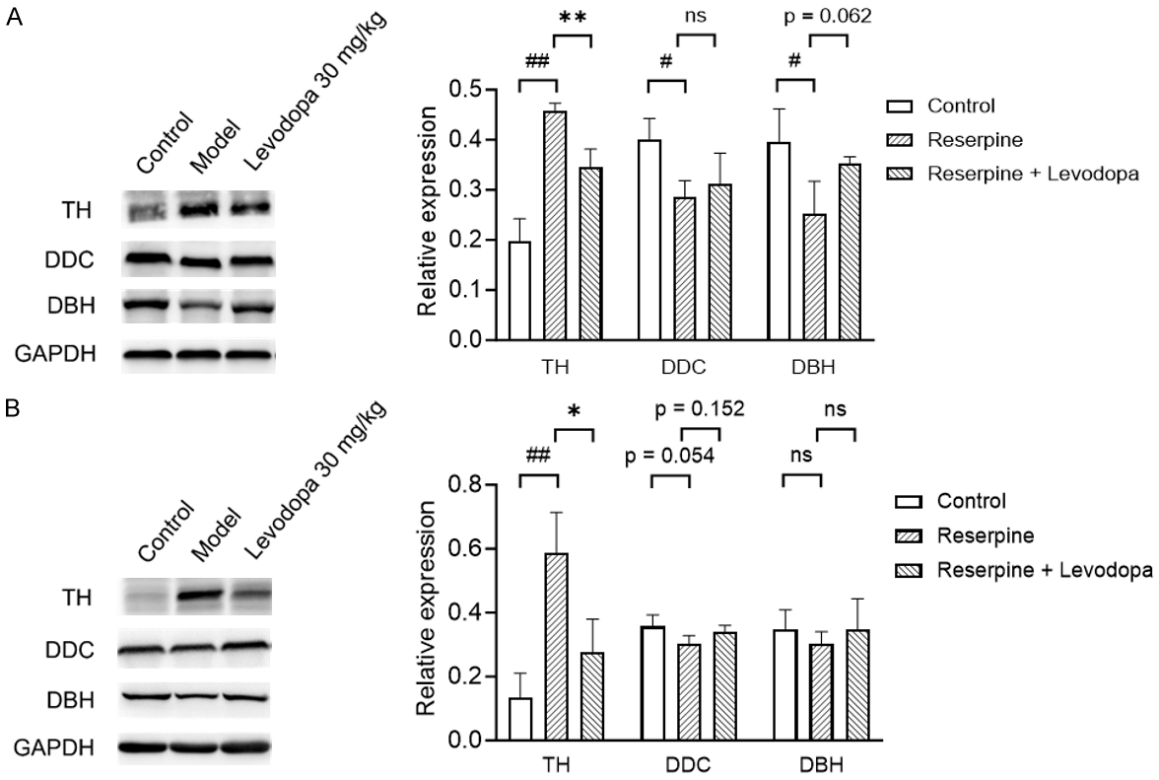

Figure 6. Effect of reserpine on NE synthetase level in cardiac and renal tissues of Wistar rats. A. Immunoblotting of TH, DDC and DBH in heart tissue; B. Immunoblotting of TH, DDC and DBH in kidney tissue. mean ± SD, n=3. $^{\#}P<0.05$, $^{\#\#}P<0.01$ *vs*. Control group; $^{*}P<0.05$, $^{**}P<0.01$ *vs*. Model group.

plasma levels of Ang II in the model group were significantly lower than those of the control group ($P<0.01$), whereas L-DOPA treatment markedly restored Ang II levels ($P<0.01$) (**Figure 8**). Consistently, plasma ALD levels also exhibited a similar downward trend in the model group and were partially reversed after L-DOPA administration. These findings suggest that reserpine-induced hypotension may be associated with suppression of the RAAS activity.

Reserpine induces a homeostatic imbalance in the NO/ET system in Wistar rats

In addition to alterations in RAAS activity, vascular endothelial regulatory systems may also contribute to the maintenance of hypotension. The NO/ET system plays a critical role in vascular and cardiovascular regulation by balancing the effects of nitric oxide (NO) and endothelin-1 (ET-1) to maintain blood pressure stability [19, 20]. NO levels were elevated in cardiac and renal tissues in the model group compared to controls ($P=0.057$; $P<0.05$) (**Figure 9A**). After L-DOPA administration, NO levels were significantly reduced relative to the model group ($P<0.05$; $P<0.05$) (**Figure 9D**). In contrast, ET-1 levels in the cardiac and renal tissues of the model group were significantly decreased compared to controls ($P<0.01$; $P<0.05$), whereas L-DOPA administration significantly increased ET-1 expression ($P<0.05$) (**Figure 9B** and **9E**). Endothelial nitric oxide synthase (eNOS) is the rate-limiting enzyme responsible for NO production [21]. eNOS expression was significantly upregulated in cardiac and renal tissues in the model group compared to the control group and was markedly downregulated after L-DOPA administration (**Figure 9C** and **9F**). Western blot further confirmed that ET-1 expression was significantly decreased in the model group and partially restored after L-DOPA administration. Collectively, these findings suggest that reserpine increases eNOS expression and NO production while decreasing ET-1 levels, leading to vasodilation and a subsequent reduction in blood pressure.

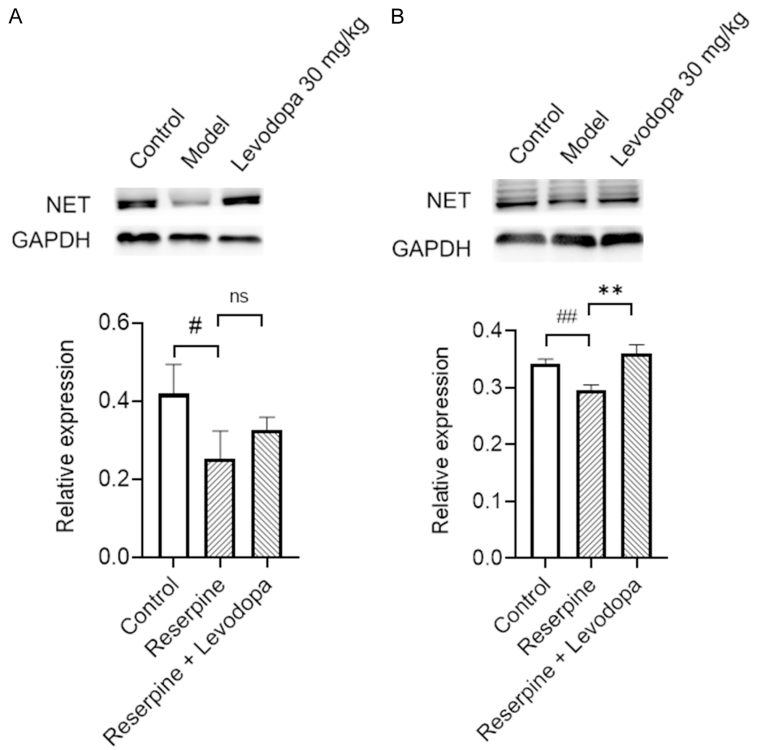

Figure 7. Effect of reserpine on NET level in cardiac and renal tissues of Wistar rats. A. Immunoblotting of NET in heart tissue; B. Immunoblotting of NET protein in kidney tissue. mean ± SD, n=3. $^{\#}P<0.05$, $^{\#\#}P<0.01$ *vs*. Control group; $^{**}P<0.01$ *vs*. Model group.

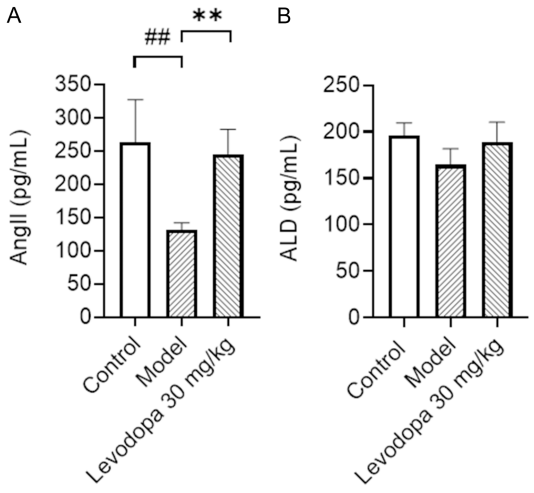

Figure 8. Effect of reserpine on Ang II and ALD levels of Wistar rats. A. Plasma Ang II level; B. Plasma ALD level. mean ± SD, n=3. $^{\#\#}P<0.01$ vs. Control group; $^{**}P<0.01$ vs. Model group.

Discussion

Reserpine-induced hypotension is attributed primarily to inhibition of sympathetic nervous system activity. Reserpine inhibits vesicular monoamine transporter, thereby blocking NE storage in synaptic vesicles and promoting rapid degradation of cytoplasmic NE by monoamine oxidase, ultimately leading to depletion of NE in sympathetic nerve terminals [22]. Decreased NE levels directly decrease peripheral vascular tone and cardiac output, leading to a reduction in blood pressure [23]. Although compensatory mechanisms may be activated, such as upregulation of TH expression to enhance NE biosynthesis, the downregulation of DDC, DBH, and NET indicates that overall NE synthesis and reuptake remain suppressed, thereby further exacerbating the hypotensive state [24].

Suppression of the sympathetic nervous system may lead to secondary inhibition of RAAS activity. Sympathetic activation stimulates renin release, thereby facilitating the generation of Ang II and ALD to maintain blood pressure homeostasis [25]. In a hypotensive state, the reduction in NE levels decreases renal sympathetic nerve activity, leading to inhibition of RAAS activation and thereby reducing compensatory vasoconstriction and sodium and water retention [26].

In addition, an imbalance of the NO/ET system represents another important mechanism contributing to blood pressure reduction. NO, a major vasodilatory mediator, promotes vascular relaxation when excessively produced, whereas ET-1, a potent vasoconstrictor, further weakens vasoconstrictive capacity when its levels decline [26]. The reserpine-induced upregulation of eNOS and NO, accompanied by reduced ET-1 expression, indicates an enhanced vasodilatory state. This alteration may represent both a compensatory response to NE depletion and a direct contributor to the further decline in blood pressure [27].

Chronic hypotension can lead to inadequate tissue perfusion, resulting in both cardiac and

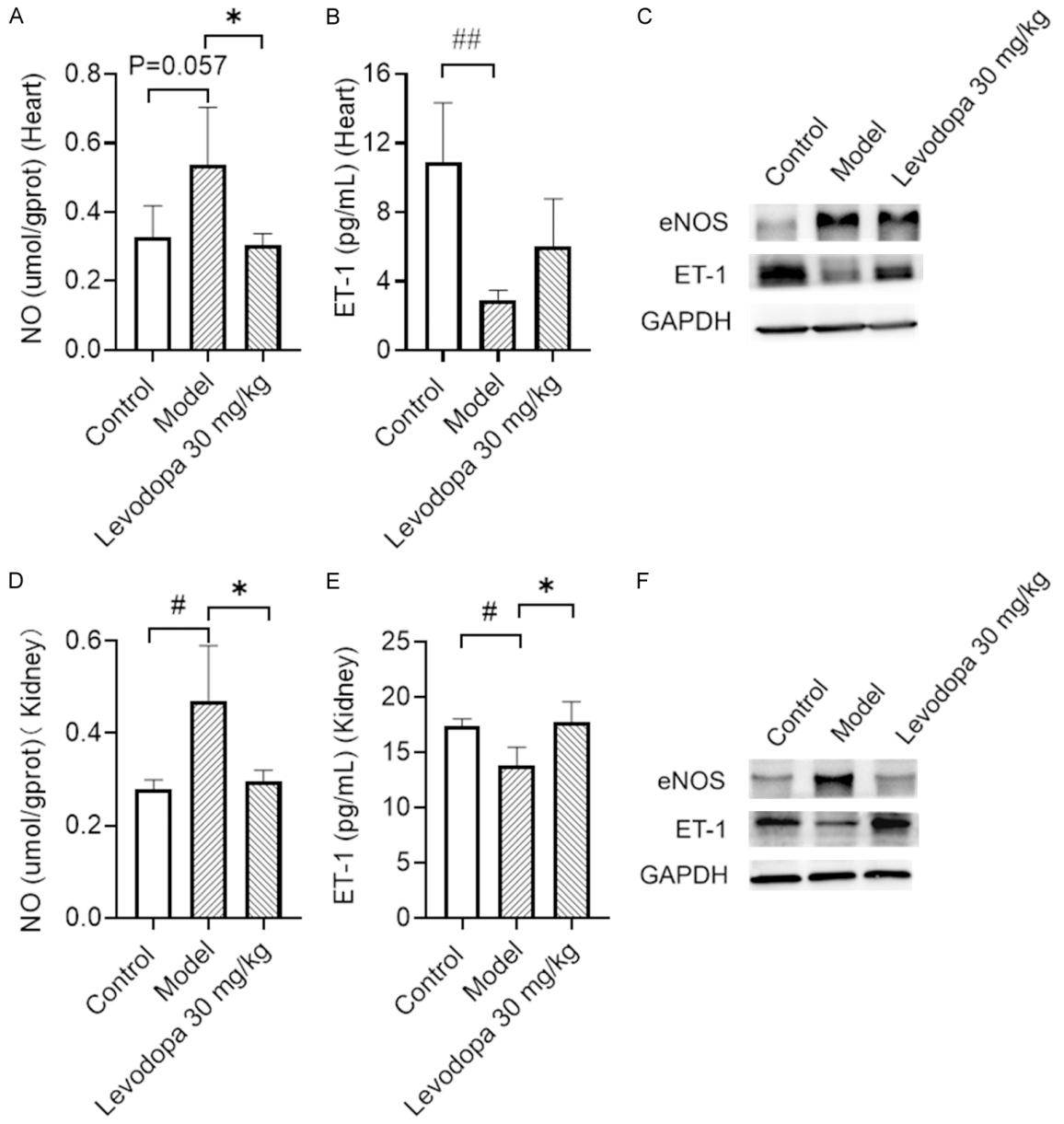

Figure 9. Effect of reserpine on the levels of NO, eNOS, and ET-1 in the heart and kidney tissues of Wistar rats. A. Heart NO level; B. Heart ET-1 level; C. Immunoblotting of eNOS and ET-1 in cardiac tissue; D. Renal NO level; E. Renal ET-1 level; F. Immunoblotting of eNOS and ET-1 proteins in renal tissue. mean ± SD, n=3. $^{\#}P<0.05$, $^{\#\#}P<0.01$ vs. Control group; $^{*}P<0.05$ vs. Model group.

renal dysfunction. The kidneys are particularly susceptible to hypoperfusion, which may induce early tubular epithelial injury characterized by cellular degeneration, nuclear loss, and epithelial detachment [28]. Notably, in the present study, no significant differences were detected in BUN or Cre levels, whereas Cys-C was significantly elevated. These findings suggest that BUN and Cre are relatively insensitive indicators of early renal injury and generally increase only after significant renal impairment has developed, whereas Cys-C is more sensitive to alterations in glomerular filtration rate [29]. Therefore, renal injury induced by early-stage hypotension may not yet have progressed to a degree detectable by BUN or Cre, while the elevation of Cys-C may already reflect mild impairment of renal function, highlighting differ-

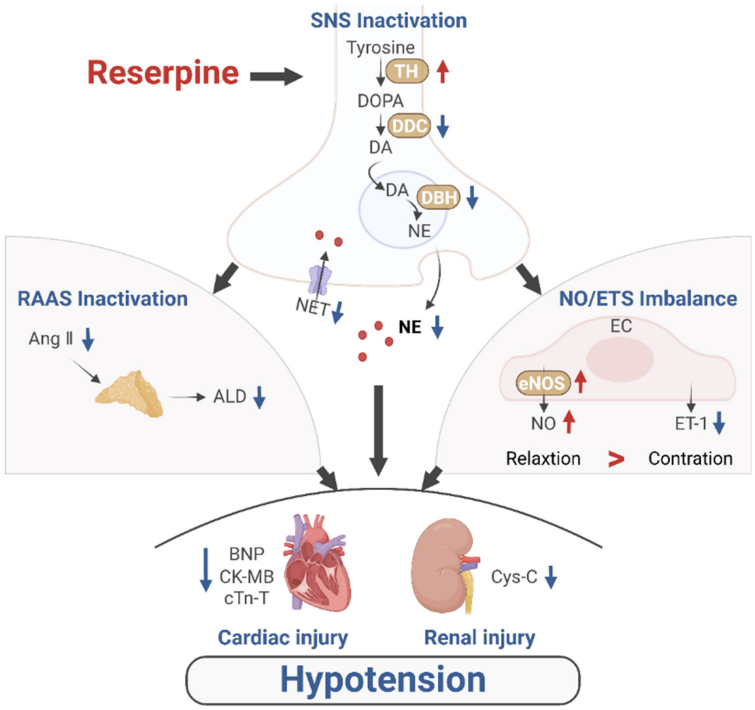

Figure 10. Possible pathologic mechanism of reserpine-induced hypotension: insight into multiple blood pressure regulatory systems.

ential sensitivities of renal biomarkers for the detection of early renal injury.

After L-DOPA administration, the levels of NE and vasoactive factors were restored, accompanied by improvements in blood pressure, cardiac and renal function. These findings suggest that restoration of sympathetic nervous system activity can partially reverse the imbalance of the RAAS and NO/ET system. Collectively, these results further support the hypothesis that inhibition of sympathetic nervous system function represents a primary upstream mechanism driving reserpine-induced hypotension, whereas alterations in the RAAS and NO/ET system are more likely secondary adaptive responses [30].

Conclusion

Collectively, the study successfully established a simple and efficient rat model of reserpine-induced hypotension that closely mimics clinical neurogenic hypotension. Furthermore, the study demonstrated that reserpine reduces blood pressure through coordinated mechanisms involving suppression of NE synthesis and reuptake, inhibition of the RAAS, and dysregulation of NO/ET system homeostasis. These findings provide an important experimental framework for mechanistic investigations and therapeutic development for neurogenic hypotension (**Figure 10**).

Acknowledgements

We would like to thank everyone involved in this project for their work. This research was supported by the Shanghai Natural Science Foundation (19ZR1413900).

Disclosure of conflict of interest

None.

Address correspondence to: Rui Wang and Jia-Wen Wang, School of Pharmacy, East China University of Science and Technology, 130 Meilong Road, Xuhui District, Shanghai 200237, P. R. China. Tel: +86-021-64250823; E-mail: ruiwang@ecust.edu.cn (RW); Tel: +86-13260192393; E-mail: m1326019-2393@163.com (JWW)

References

[1] Chen RJ, Sharma S and Bhattacharya PT. Hypotension. Treasure Island (FL): StatPearls Publishing; 2026. pp. 1-15.

[2] Cheng Y, Lin L, Huang P, Zhang J, Wang Y and Pan X. Hypotension with neurovascular changes and cognitive dysfunction: an epidemiological, pathobiological, and treatment review. Chin Med J (Engl) 2025; 138: 405-418.

[3] Mills KT, Stefanescu A and He J. The global epidemiology of hypertension. Nat Rev Nephrol 2020; 16: 223-237.

[4] Unger T, Borghi C, Charchar F, Khan NA, Poulter NR, Prabhakaran D, Ramirez A, Schlaich M, Stergiou GS, Tomaszewski M, Wainford RD, Williams B and Schutte AE. 2020 International Society of hypertension global hypertension practice guidelines. Hypertension 2020; 75: 1334-1357.

[5] Mizuno T, Hayashi T, Shimabukuro Y, Murase M, Hayashi H, Ishikawa K, Takahashi K, Yuzawa Y, Yamada S and Nagamatsu T. Lower blood pressure-induced renal hypoperfusion promotes cisplatin-induced nephrotoxicity. Oncology 2016; 90: 313-320.

[6] Ma J, Li Y, Yang X, Liu K, Zhang X, Zuo X, Ye R, Wang Z, Shi R, Meng Q and Chen X. Signaling pathways in vascular function and hypertension: molecular mechanisms and therapeutic interventions. Signal Transduct Target Ther 2023; 8: 168.
[7] Mwesigwa N and Shibao CA. Norepinephrine reuptake inhibition, an emergent treatment for neurogenic orthostatic hypotension. Hypertension 2024; 81: 1460-1466.
[8] Jung YJ, Kim A, Okamoto LE and Hong WH. Effects of atomoxetine for the treatment of neurogenic orthostatic hypotension in patients with alpha-synucleinopathies: a systematic review of randomized controlled trials and a focus-group discussion. J Clin Neurol 2023; 19: 165-173.
[9] Biaggioni I. New developments in the management of neurogenic orthostatic hypotension. Curr Cardiol Rep 2014; 16: 542.
[10] Hauser RA, Favit A, Hewitt LA, Lindsten A, Gorny S, Kymes S and Isaacson SH. Durability of the clinical benefit of droxidopa for neurogenic orthostatic hypotension during 12 weeks of open-label treatment. Neurol Ther 2022; 11: 459-469.
[11] Strawbridge R, Javed RR, Cave J, Jauhar S and Young AH. The effects of reserpine on depression: a systematic review. J Psychopharmacol 2023; 37: 248-260.
[12] Zhang X, Wang C, Zhang ZY, Zhang PP, Ren Q, Wang XL and Mao JY. Establishment of a rat model of hypotension induced by reserpine. Zhongguo Yi Xue Ke Xue Yuan Xue Bao 2023; 45: 533-540.
[13] Lorenzen JM, Batkai S and Thum T. Regulation of cardiac and renal ischemia-reperfusion injury by microRNAs. Free Radic Biol Med 2013; 64: 78-84.
[14] Odudu A and McIntyre CW. An update on intradialytic cardiac dysfunction. Semin Dial 2016; 29: 435-441.
[15] Shamon SD and Perez MI. Blood pressure-lowering efficacy of reserpine for primary hypertension. Cochrane Database Syst Rev 2016; 12: CD007655.
[16] Ames MK, Atkins CE and Pitt B. The renin-angiotensin-aldosterone system and its suppression. J Vet Intern Med 2019; 33: 363-382.
[17] Ghazi L and Drawz P. Advances in understanding the renin-angiotensin-aldosterone system (RAAS) in blood pressure control and recent pivotal trials of RAAS blockade in heart failure and diabetic nephropathy. F1000Res 2017; 6: 297.
[18] King VL, English VL, Bharadwaj K and Cassis LA. Angiotensin II stimulates sympathetic neurotransmission to adipose tissue. Physiol Rep 2013; 1: e00014.
[19] Godo S and Shimokawa H. Endothelial functions. Arterioscler Thromb Vasc Biol 2017; 37: e108-e114.
[20] Davenport AP, Hyndman KA, Dhaun N, Southan C, Kohan DE, Pollock JS, Pollock DM, Webb DJ and Maguire JJ. Endothelin. Pharmacol Rev 2016; 68: 357-418.
[21] Ghasemi A and Jeddi S. Quantitative aspects of nitric oxide production in the heart. Mol Biol Rep 2022; 49: 11113-11122.
[22] Fernandez CJ, Hanna FW, Pacak K and Nazari MA. Catecholamines and blood pressure regulation. Endocrine 2023; 19-34.
[23] Souza LAC and Earley YF. (Pro)renin receptor and blood pressure regulation: a focus on the central nervous system. Curr Hypertens Rev 2022; 18: 101-116.
[24] Pan HC, Yang SY, Chiou TT, Shiao CC, Wu CH, Huang CT, Wang TJ, Chen JY, Liao HW, Chen SY, Huang TM, Yang YF, Lin HY, Chan MJ, Sun CY, Chen YT, Chen YC and Wu VC. Comparative accuracy of biomarkers for the prediction of hospital-acquired acute kidney injury: a systematic review and meta-analysis. Crit Care 2022; 26: 349.
[25] Ostermann M, Legrand M, Meersch M, Srisawat N, Zarbock A and Kellum JA. Biomarkers in acute kidney injury. Ann Intensive Care 2024; 14: 145.
[26] Jana S, Mitra P and Roy S. Proficient novel biomarkers guide early detection of acute kidney injury: a review. Diseases 2022; 11: 8.
[27] Ajoolabady A, Pratico D and Ren J. Endothelial dysfunction: mechanisms and contribution to diseases. Acta Pharmacol Sin 2024; 45: 2023-2031.
[28] Carlström M, Weitzberg E and Lundberg JO. Nitric oxide signaling and regulation in the cardiovascular system: recent advances. Pharmacol Rev 2024; 76: 1038-1062.
[29] Grassi G, Dell'Oro R, Quarti-Trevano F, Vanoli J and Oparil S. Sympathetic neural mechanisms in hypertension: recent insights. Curr Hypertens Rep 2023; 25: 263-270.
[30] Inker LA, Eneanya ND, Coresh J, Tighiouart H, Wang D, Sang Y, Crews DC, Doria A, Estrella MM, Froissart M, Grams ME, Greene T, Grubb A, Gudnason V, Gutiérrez OM, Kalil R, Karger AB, Mauer M, Navis G, Nelson RG, Poggio ED, Rodby R, Rossing P, Rule AD, Selvin E, Seegmiller JC, Shlipak MG, Torres VE, Yang W, Ballew SH, Couture SJ, Powe NR and Levey AS; Chronic Kidney Disease Epidemiology Collaboration. New creatinine- and cystatin C-based equations to estimate GFR without race. N Engl J Med 2021; 385: 1737-1749.